Clinical Research in Cardiology (2019) 108:1147–1162
https://doi.org/10.1007/s00392-019-01450-w

ORIGINAL PAPER

Biventricular myocardial strain analysis using cardiac magnetic resonance feature tracking (CMR-FT) in patients with distinct types of right ventricular diseases comparing arrhythmogenic right ventricular cardiomyopathy (ARVC), right ventricular outflow-tract tachycardia (RVOT-VT), and Brugada syndrome (BrS)

Philipp Heermann[1] · H. Fritsch[5] · M. Koopmann[3] · P. Sporns[2] · M. Paul[4] · W. Heindel[2] · E. Schulze-Bahr[5] · C. Schülke[2]

Received: 29 November 2018 / Accepted: 5 March 2019 / Published online: 13 March 2019

Abstract

Objectives As underlying heart diseases of right ventricular tachyarrhythmias, ARVC causes wall-motion abnormalities based on fibrofatty myocardial degeneration, while RVOT-VT and BrS are thought to lack phenotypic MR characteristics. To examine whether cardiac magnetic resonance (CMR) feature tracking (FT) in addition to ARVC objectively facilitates detection of myocardial functional impairments in RVOT-VT and BrS.

Methods Cine MR datasets of four retrospectively enrolled, age-matched study groups [$n=65$; 16 ARVC, 26 RVOT-VT, 9 BrS, 14 healthy volunteers (HV)] were independently assessed by two distinctly experienced investigators regarding myocardial function using CMR-FT. Global strain (%) and strainrate (s^{-1}) in radial and longitudinal orientation were assessed at RVOT as well as for left (LV) and right (RV) ventricle at a basal, medial and apical section with the addition of a biventricular circumferential orientation.

Results RV longitudinal and radial basal strain (%) in ARVC (-12.9 ± 4.2; 11.4 ± 5.1) were significantly impaired compared to RVOT-VT (-18.0 ± 2.5, $p\leq0.005$; 16.4 ± 5.2, $p\leq0.05$). Synergistically, RVOT endocardial radial strain (%) in ARVC (33.8 ± 22.7) was significantly lower ($p\leq0.05$) than in RVOT-VT (54.3 ± 14.5). For differentiation against BrS, RV basal and medial radial strain values (%) (13.3 ± 6.1; 11.8 ± 2.9) were significantly reduced when compared to HV (21.0 ± 6.9, $p\leq0.05$; 20.1 ± 6.6, $p\leq0.005$), even in case of a normal RV ejection fraction (EF) (>45%; $n=6$) (12.0 ± 2.7 vs. 20.1 ± 6.6, $p\leq0.05$).

Conclusions CMR-FT facilitates relevant differentiation in patients with right ventricular tachyarrhythmias: between ARVC against RVOT-VT and HV as well as between BrS with even a preserved EF against HV.

Keywords Feature tracking (FT) · Myocardial strain analysis · Arrhythmogenic right ventricular cardiomyopathy (ARVC) · Brugada syndrome (BrS) · Right ventricular outflow tract tachycardia (RVOT-VT)

Abbreviations

ARVC	Arrhythmogenic right ventricular cardiomyopathy
AUC	Area under curve
BrS	Brugada syndrome
CMR	Cardiac magnetic resonance
DSC-2	Desmocolin-2
DSG-2	Desmoglein-2
EF	Ejection fraction
FT	Feature tracking
LV	Left ventricle left ventricular
LVEDVI	Left ventricular end diastolic volume index
LVEF	Left ventricular ejection fraction
LVESVI	Left ventricular end systolic volume index
PKP-2	Plakophillin-2
ROC	Receiver operating curve
RV	Right ventricle/right ventricular
RVEDVI	Right ventricular end diastolic volume index
RVEF	Right ventricular ejection fraction
RVESVI	Right ventricular end systolic volume index
RVOT	Right ventricular outflow tract

E. Schulze-Bahr and C. Schülke are co-contributing senior authors.

✉ Philipp Heermann
philipp.heermann@gmx.de

Extended author information available on the last page of the article

RVOT-VT	Right ventricular outflow tract tachycardia
SA	Short axis
SCD	Sudden cardiac death
SCN5A	Ion channel mutation in Brugada syndrome
SD	Standard deviation
TFS	Task Force Score
WMA	Wall-motion abnormalities
4 CH	Four chamber

Introduction

Implicating the risk of right ventricular (RV) tachyarrhythmias and sudden cardiac death (SCD) predominantly in young people constitutes a common characteristic of arrhythmogenic rightventricular cardiomyopathy (ARVC), right ventricular outflow tract tachycardia (RVOT-VT) and Brugada syndrome (BrS) [1–6].

ARVC is characterized by progressive fibrofatty degeneration and replacement of predominantly right ventricular myocardium [1, 7]. Nonetheless, ARVC diagnosis is not solely established on histopathological information but based on a set of diagnostic Task Force Criteria (TFC) arising from numerous diagnostic procedures [8] that have been revised in 2010 [3]. Not least because of this determining modification cardiovascular magnetic resonance (CMR) imaging is nowadays predominantly used in the diagnostic workup of suspected ARVC and other cardiomyopathies, but additionally due to a reliable and reproducible quantification of RV dimensions and a capable detection of fatty tissue and scar formation within myocardial layers [1, 9–11].

Arising from this background, we examined the capability of CMR-based strain as a novel technique to objectively measure global and regional ventricular dysfunction in ARVC patients in our recently published study [12], as prior echocardiographic based strain studies already had underlined a trend towards increased observer-independence [13, 14] and ascendency of strain imaging against established measurements of early forms of myocardial dysfunction [15–20].

RVOT-VT is characterized by ventricular tachyarrhythmias of left bundle branch block (LBBB) arising from the RVOT in the setting of a preserved ejection fraction. Its diagnosis is obtained by excision of pathomorphological tissue characteristics [6, 21]. In contrast to ARVC, RVOT-VT is not classified as a cardiomyopathy. To date, only little is known on the cause of RVOT-VTs; however, these may be in part genetically determined [22].

Likewise, Brugada syndrome (BrS) is associated with an increased incidence of cardiac events due to ventricular arrhythmias and supposed to be unrelated to identifiable distinct structural myocardial changes [4, 5, 23, 24]. It is a genetically determined ion channel disorder resulting in characteristic ECG changes and ST-segment elevations in one or more right precordial leads [4, 25, 26].

A portion of BrS patients may have substructural abnormalities consistent with fibrosis in the RVOT, as CMR-based mild structural RV changes on a conventional qualitative and quantitative scope have been reported [27, 28] and performance of echocardiographic based strain using 2D speckle tracking analysis in BrS has been examined [29].

The role of strain imaging in CMR is constantly increasing, as retrospective derivation of strain parameters from conventional cine CMR using a feature tracking (FT) algorithm is implemented [30, 31]. Numerous studies propose that this novel technique might play a role in early and objective detection of myocardial functional impairments of various cardiac pathologies [32–38], remarkably likewise of predominantly RV-contraction abnormalities [12, 39, 40].

In sequel of our recently outlined study conclusion for CMR feature tracking [12], the aim of the present study was to examine the diagnostic performance of biventricular CMR-based feature tracking in the domain of delineated differential diagnoses of RV tachyarrhythmias. In detail, we investigated whether CMR-FT objectively facilitates detection of myocardial functional impairments in RVOT-VT and BrS in addition to ARVC and particularly enables differentiation between ARVC against RVOT-VT and BrS against HV. As being part of the triangle of dysplasia, we additionally examined the diagnostic performance of CMR feature tracking ascertained at this potentially promising anatomic landmark in RV tachyarrhythmias.

Methods

Study population

With approval of the local ethics committee, this retrospective CMR study was performed on 69 individuals that had been referred to our department for CMR imaging either due to suspicious ARVC according to the major and minor TFC ($n=20$), for exclusion of structural heart disease in the setting of RVOT-VT ($n=26$) or for exclusion of phenocopies mimicking BrS (e.g., RVOT compression) in patients with a Brugada type-1-ECG according to current criteria ($n=9$) [4]. CMR images of 14 healthy volunteers (HV) served as the control group. Study groups have been matched for age within the process of inclusion. Prior to CMR imaging, written informed consent concerning the clinically indicated examination was acquired from all subjects.

Final diagnosis of ARVC was reassessed by appraisal according to the 2010 TFC [41] concerning presence of revised minor and major criteria and newly supplemented quantitative cutoff values. Correspondingly, diagnosis was established if two major, one major plus two minor or four

minor criteria from different categories were present [41]. Diagnosis of ARVC was finally confirmed in 16 out of 20 initially referred patients suspicious of ARVC resulting in a total inclusion of 65 patients in the study. RVOT-VT finally was diagnosed by exclusion of pathomorphological myocardial characteristics by CMR in addition to presence of delineated tachyarrhythmias arising from RVOT. Clinical features of the study groups are listed in Table 1.

Cardiac MR (CMR) imaging

All CMR scans were performed on a 1.5-Tesla system (Achieva, Philips, Best, The Netherlands). A retrospectively ECG-triggered balanced steady-state free precession (b-SSFP) sequence in breath-hold technique was performed for conventional functional analysis by acquisition of short axis (SA) orientation covering the entire LV and axial orientation covering the complete RV, respectively. In addition to SA, a 4-chamber (4-CH) orientation was acquired for consecutive CMR-FT analysis. Imaging parameters were adjusted as follows: echo time (TE) and repetition time (TR) were set to shortest leading to an average TR of 4 ms and a TE of 2 ms slightly varying with slice orientation. 25 phases per cardiac cycle were acquired. The obtained in-plane resolution depended on the field of view (set according to patient's constitution) with a mean reconstructed pixel size of 1.7 ± 0.2 mm × 1.5 ± 0.2 mm. Slice thickness of b-SSFP images was 6 mm for both axial and short axis planes.

Cine images were assessed qualitatively for the presence of RV regional wall-motion abnormalities (WMA) by two experienced observers in consensus in addition to quantitative volumetric analysis.

Both readers were blinded to clinical data and independently read the datasets in random order. Data preparation was performed by a person not involved in the reading process.

CMR-based strain analysis using feature tracking

CMR-FT analysis based on the acquired b-SSFP cine images was performed by the application of a specialized software with capability of myocardial deformation analysis (Circle Cardiovascular Imaging cvi[42], Canada and The Netherlands). The technical details of retrospective derivation of

Table 1 Basic demographics, volumetric data, and characteristics of patients

	Healthy volunteers	ARVC	RVOT-VT	BrS
n	14	16	26	9
Sex (m/w)	9/5	14/2	12/14	6/3
Age	48.8 ± 14.1	60.1 ± 15.5	55.6 ± 11.1	46.8 ± 10.2
Weight	83.0 ± 18.1	82.9 ± 17.6	79.5 ± 13.9	76.9 ± 10.4
Height	173.2 ± 14.4	178.9 ± 7.7	175.0 ± 9.2	175.7 ± 10.2
Body surface area	2.0 ± 0.3	2.0 ± 0.2	1.9 ± 0.2	1.9 ± 0.2
RVEDVI (ml/m^2)	77.2 ± 21.2	122.7 ± 37.1***$^{\#\#\$}$	91.2 ± 18.9	89.1 ± 17.2
RVESVI (ml/m^2)	32.6 ± 9.5	76.3 ± 35.6***$^{\#\#\#\$\$}$	43.3 ± 12.6	46.9 ± 12
RVEF (%)	57.5 ± 2.6	40.4 ± 10.2***$^{\#\#\#}$	53.0 ± 6.5	47.9 ± 5.9*
RVEF > 40/RVEF < 40 (%)	14/0	9/7	26/0	9/0
LVEDVI (ml/m^2)	71.6 ± 17.5	86.7 ± 19.9	89.0 ± 22.0	81.4 ± 6.7
LVESVI (ml/m^2)	28.2 ± 10.0	35.9 ± 15.7	38.4 ± 25.5	33.6 ± 5.5
LVEF	61.3 ± 5.7	60.1 ± 10.0	61.0 ± 7.2	58.6 ± 5.8
TFS	0	5.8 ± 1.4	0	0
WMA	14/0/0/0/0	3/0/1/4/8	26/0/0/0/0	9/0/0/0/0
Genetic evaluation	0	9 (PKP2+)	0	3 (SCN5A+)
Brugada Type-1-ECG	0	0	0	9

WMA is graded in the following order no WMA/hypokinesia/akinesia/dyskinesia/aneurysm. Mutations: ARVC—Plakophillin-2 (PKP-2) or Desmoglein-2 (DSG-2) or Desmocolin-2 (DSC-2), BrS—SCN5A

ARVC arrhythmogenic right ventricular cardiomyopathy, *RVOT-VT* right ventricular outflow tract tachycardia, *BrS* Brugada syndrome, *RVEDVI* right ventricular end diastolic volume index, *RVESVI* right ventricular end systolic volume index, *RVEF* right ventricular ejection fraction, *LVEDVI* left ventricular end diastolic volume index, *LVESVI* left ventricular end systolic volume index, *LVEF* left ventricular ejection fraction, *TFS* task force score, *WMA* wall-motion abnormalities

Level of significance $^{*,\#,\$}p < 0.05$, $^{**,\#\#,\$\$}p < 0.01$, $^{***,\#\#\#,\$\$\$}p < 0.005$

*Significant difference compared to healthy volunteers;

$^{\#}$Significant difference compared to patients with RVOT-VT

$^{\$}$Significant difference compared to patients with BrS

strain parameters from conventional cine CMR sequences using a feature tracking algorithm have been implemented and published previously [30, 31]. 4-CH view was used to derive LV and RV longitudinal strain and strainrate values (Fig. 1a). LV and RV radial and circumferential strain and strainrate parameters were evaluated in SA view at a basal, a medial, and an apical section of the ventricle (Fig. 1c), respectively.

To guarantee standardized and reproducible strain analysis in all subjects, the basal myocardial layer for deformation analysis was defined as the first slice below the atrioventricular level revealing a circumferential myocardia enclosing throughout all heartphases, the medial myocardial layer was determined to be localized at the level of both papillary muscles and the apical myocardial layer to measure deformation was set to the equidistance of basal and medial myocardial layers in direction towards the apex.

RVOT radial and longitudinal strain and strainrate parameters were derived accordingly; by definition the RVOT layer was the first slice below pulmonary valve level revealing a closed oval configuration in an axial view (Fig. 1b) throughout all heartphases.

For CMR-FT analysis (Fig. 1), epicardial and endocardial contours for both ventricles at the defined sections and endocardial contours for RVOT at the determined level were drawn manually in end-systolic images by two independent readers (R1 with 7 years experience in CMR; R2 without previous experience) to initiate the software-based automatic tracking of the respective contours throughout the entire cardiac cycle. The quality of automatic tracking was evaluated and contours were manually adjusted if necessary.

Statistical analysis

Statistical analysis was based on SPSS 23 software package (IBM). Analysed data are demonstrated as mean ± standard deviation. To test for significant differences between presented study groups as well as between subgroups of study groups categorized by ejection fraction (EF) cutoff values analysis of variance (ANOVA) testing was performed. For post-hoc analysis of multiple paired-group comparisons, Bonferroni correction was applied predominantly, whereas in rare cases of inhomogenous distribution of variances Dunnett-T3 testing was used.

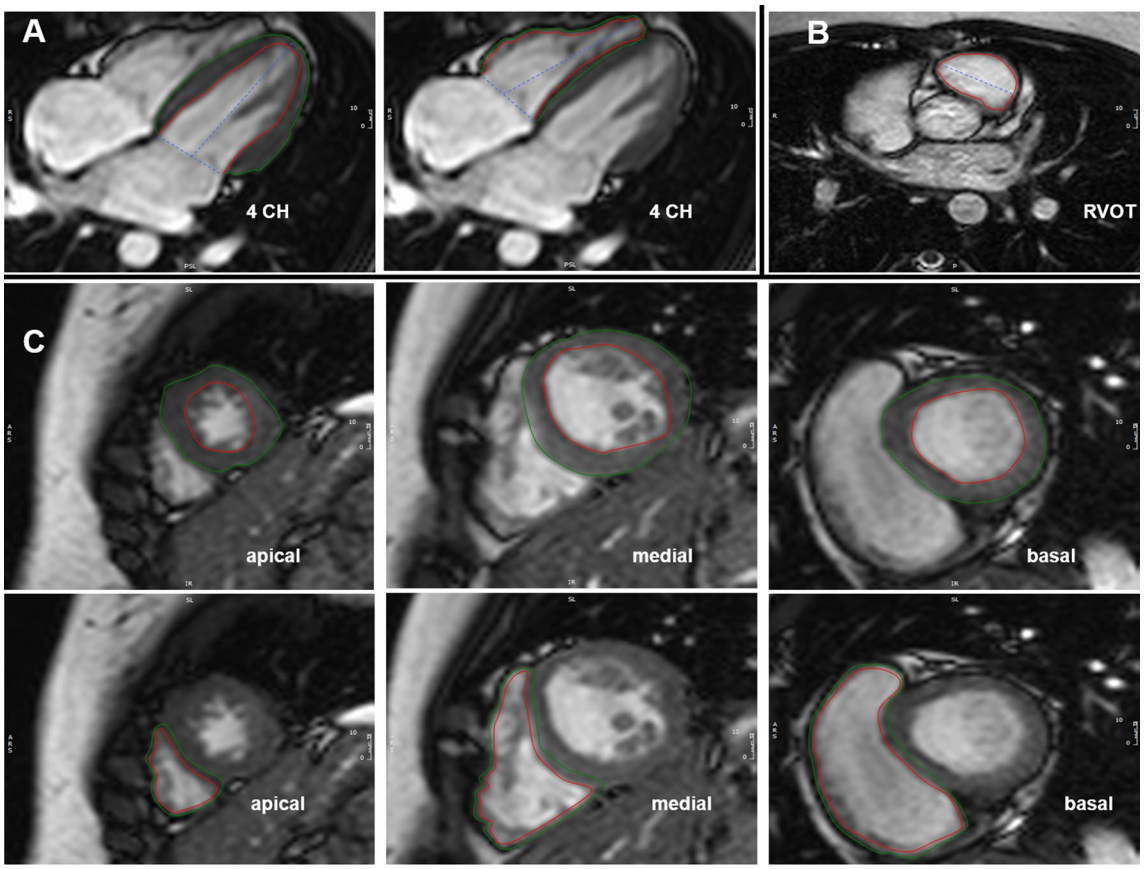

Fig. 1 Tracked left (LV) and right ventricular (RV) epicardial (green) and endocardial (red) contours in 4-CH (**a**) and SA (**c**) at the apical, medial and basal level as well as tracked endocardial contour (red) at the RVOT (**b**)

For all patients with ARVC or BrS a subgroup analysis was assessed according to EF with graduation based on the defined cutoff values of the 2010 TFC [3], in case of ARVC according to the cutoff value for major criterion (EF < 40%), in case of BrS according to the cutoff value for minor criterion (EF < 45%).

Using receiver operating curve (ROC) analysis we evaluated diagnostic accuracy of RV global conventional functional (EF) and strain parameters for all patients with diagnosis of ARVC ($n = 16$) based on ≥ 4 points in 2010 TFC (major criteria = 2 points, minor criteria = 1 point) as the gold standard in comparison to healthy volunteers and RVOT-VT. Analogously, we evaluated diagnostic accuracy of corresponding RV parameters for all patients with diagnosis of BrS ($n = 9$) based on the detection of Brugada type-1-ECG as the gold standard in comparison to healthy volunteers and ARVC.

In addition, we performed corresponding ROC analysis of LV EF and strain parameters for comparisons between HV and ARVC or BrS.

Optimal cutoff values were identified to achieve a high sensitivity and a reasonable high specificity for detection of disease. A p value of < 0.05 was classified as statistically significant.

For statistical analysis of interobserver agreement and objectivity of CMR-FT according to RV and RVOT strain analysis almost all individuals of the delineated four study groups ($n = 57$) were evaluated by two distinctly experienced readers (PH experienced; HF unexperienced) independently and blinded to clinical information, respectively. Interobserver comparisons of representative RV and RVOT strain parameters were statistically appraised by Pearson's r correlation and statistically visualized by Bland–Altman plot, respectively.

Results

Basic demographic and volumetric data

Demographic characteristics and basic diagnostic data of the four age-matched study groups are presented in Table 1.

In ARVC patients, RV enddiastolic volume index (RVEDVI) and RV end systolic volume index (RVESVI) were significantly increased compared to all other study groups. RVEF both in ARVC and in BrS was significantly reduced compared to HV. In contrast, LV volumetric data did not differ significantly between the four groups.

CMR-based strain analysis using feature tracking

All RV and LV global strain and strainrate parameters are demonstrated in Table 2. RV longitudinal (Fig. 2) and basal radial (Fig. 3) strain (%) values in patients with ARVC (-12.9 ± 4.2; 11.4 ± 5.1) were significantly decreased in comparison to patients with RVOT-VT (-18.0 ± 2.5, $p \leq 0.005$; 16.4 ± 5.2, $p \leq 0.05$) and to HV (-20.1 ± 3.7; 21.0 ± 6.9, $p \leq 0.005$), respectively, whereas a significant differentiation between RVOT-VT and HV concerning corresponding parameters was not feasible.

Synergistically, assessed RVOT endocardial radial strain (Fig. 4) and strainrate values in ARVC ($33.8 \pm 22.7\%$; $1.86 \pm 1.18\ s^{-1}$) were significantly impaired ($p \leq 0.05$) compared to RVOT-VT ($54.3 \pm 14.5\%$; $2.99 \pm 0.94\ s^{-1}$) (Table 3).

In addition, RV longitudinal strain (Fig. 2) in ARVC ($-12.9 \pm 4.2\%$) was significantly lower ($p \leq 0.05$) compared to BrS ($-16.9 \pm 2.8\%$).

Regarding further differentiation against BrS, RV radial strain values (%) at the basal (13.3 ± 6.1) (Fig. 3) and medial (11.8 ± 2.9) sections were significantly reduced compared with HV (21.0 ± 6.9, $p \leq 0.05$; 20.1 ± 6.6, $p \leq 0.005$).

For statistical analyses of RV circumferential strains, values at the defined basal section both in ARVC ($-7.8 \pm 3.7\%$) and in BrS ($-7.3 \pm 7.5\%$) were significantly reduced ($p \leq 0.05$) compared to HV ($-12.9 \pm 4.4\%$) and corresponding values at the defined medial section in ARVC ($-8.1 \pm 4.5\%$) were significantly decreased ($p \leq 0.005$) in comparison to HV ($-12.8 \pm 3.3\%$).

Further RV global strain and corresponding strainrate data as well as consecutive statistical relations among the 4 study groups are demonstrated in Table 2.

Despite corresponding LV volumetric data not differing significantly between the study groups, LV strain values proved to be significantly different ($p \leq 0.05$) concerning LV longitudinal strain (%) in comparison of ARVC (-15.9 ± 2.5) and HV (-19.3 ± 2.4) as well as regarding LV basal radial strain (%) in comparison of BrS (24.1 ± 5.5) and HV (32.7 ± 7) (Table 2).

Subgroup analysis

RV global longitudinal strain ($-14.6 \pm 3.1\%$) and RV basal radial strain ($13.8 \pm 3.5\%$) in patients with ARVC and a simultaneously slightly decreased or preserved RVEF (> 40%; $n = 9$) was significantly reduced ($p < 0.01$; $p < 0.05$) in comparison to corresponding values (%) of HV (-20.1 ± 3.7; 21.0 ± 6.9) (Table 4) [12].

Beyond that, data of the actual study demonstrated that in the subgroup of patients with ARVC with RVEF > 40% ($n = 9$) RV longitudinal strain (%) (-14.6 ± 3.1) was even more significantly reduced when compared to patients with RVOT-VT (-18.0 ± 2.5, $p \leq 0.05$) (Fig. 5; Table 4).

Regarding differentiation of BrS within an EF-based subgroup graduation, RV medial radial strain (%) (12.0 ± 2.7) in BrS with preserved RVEF (> 45%; $n = 6$) was significantly

Table 2 Comparison of right and left ventricular strain and strainrate parameters between healthy volunteers, ARVC, RVOT-VT, and BrS

	Healthy volunteers	ARVC	RVOT-VT	BrS
RV strain (%)				
Longitudinal	− 20.1 ± 3.7	− 12.9 ± 4.2***$^{\#\#\#\$}$	− 18.0 ± 2.5	− 16.9 ± 2.8
Circumferential				
Basal	− 12.9 ± 4.4	− 7.8 ± 3.7*	− 9.3 ± 2.9	− 7.3 ± 7.5*
Medial	− 12.8 ± 3.3	− 8.1 ± 4.5***	− 8.5 ± 3.2***	− 9.4 ± 2
Apical	− 16.4 ± 6.5	− 14.6 ± 6.9	− 14.3 ± 3.5	− 10.9 ± 4.1
Radial				
Basal	21.0 ± 6.9	11.4 ± 5.1***$^{\#}$	16.4 ± 5.2	13.3 ± 6.1*
Medial	20.1 ± 6.6	13.6 ± 9.4	13.4 ± 5.3 *	11.8 ± 2.9***
Apical	30.6 ± 16.1	24.7 ± 13.3	26.1 ± 13.1	15.4 ± 6.6
RV strainrate (1/s)				
Longitudinal	− 2.16 ± 1.82	− 1.06 ± 0.81	− 1.51 ± 1.01	− 1.11 ± 0.20
Circumferential				
Basal	− 1.21 ± 0.95	− 0.54 ± 0.18***	− 0.74 ± 0.29*	− 0.73 ± 0.22
Medial	− 0.88 ± 0.38	− 0.54 ± 0.21	− 0.77 ± 0.40	− 0.74 ± 0.30
Apical	− 1.68 ± 1.06	− 0.94 ± 0.44	− 1.18 ± 0.68	− 1.21 ± 0.42
Radial				
Basal	1.68 ± 1.11	0.78 ± 0.35***	1.08 ± 0.38*	0.92 ± 0.33
Medial	1.55 ± 1.07	0.87 ± 0.53*	1.06 ± 0.51	1.03 ± 0.38
Apical	1.94 ± 0.93	1.72 ± 0.91	1.59 ± 0.83	1.68 ± 0.59
LV strain (%)				
Longitudinal	− 19.3 ± 2.4	− 15.9 ± 2.5*	− 17.3 ± 2.2	− 17.3 ± 3.7
Circumferential				
Basal	− 17.8 ± 3.4	− 15.2 ± 2.8	− 14.4 ± 2.1*	− 14.9 ± 2.7
Medial	− 17.1 ± 4.1	− 15.7 ± 4.1	− 15.2 ± 2.8	− 14.5 ± 3.1
Apical	− 22.0 ± 5.3	− 19.7 ± 4.3	− 19.8 ± 3.7	− 18.0 ± 2.5
Radial				
Basal	32.7 ± 7	26.5 ± 6.8	25.5 ± 5.8*	24.1 ± 5.5*
Medial	29.1 ± 9	27.0 ± 11.0	23.8 ± 6	23.0 ± 7.5
Apical	45.4 ± 19.2	40.6 ± 20.1	39.1 ± 12.6	32.8 ± 7.7
LV strainrate (1/s)				
Longitudinal	− 1.22 ± 0.31	− 0.93 ± 0.18*	− 0.95 ± 0.17*	− 1.13 ± 0.26
Circumferential				
Basal	− 0.93 ± 0.18	− 0.79 ± 0.16	− 0.79 ± 0.14	− 0.91 ± 0.15
Medial	− 1.06 ± 0.31	− 0.85 ± 0.18	− 0.89 ± 0.17	− 1.12 ± 0.22
Apical	− 1.43 ± 0.39	− 1.32 ± 0.55	− 1.44 ± 0.49	− 1.95 ± 0.54

Table 2 (continued)

	Healthy volunteers	ARVC	RVOT-VT	BrS
Radial				
Basal	2.0 ± 0.60	1.31 ± 0.56*	1.28 ± 0.35*	1.56 ± 0.36
Medial	1.87 ± 0.72	1.39 ± 0.34	1.34 ± 0.35*	1.65 ± 0.44
Apical	2.85 ± 1.31	1.93 ± 0.58	2.40 ± 0.95	2.61 ± 0.94

ARVC arrhythmogenic right ventricular cardiomyopathy, *RVOT-VT* right ventricular outflow tract tachycardia, *BrS* Brugada syndrome

Level of significance $^{*,\#,\$}p<0.05$, $^{**,\#\#,\$\$}p<0.01$, $^{***,\#\#\#,\$\$\$}p<0.005$

*Significant difference compared to healthy volunteers

#Significant difference compared to patients with RVOT-VT

$Significant difference compared to patients with BrS

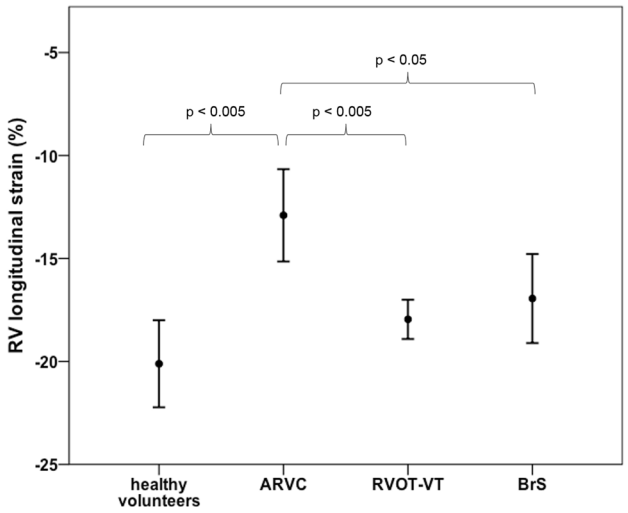

Fig. 2 Comparison of RV longitudinal strain between HV and patient groups

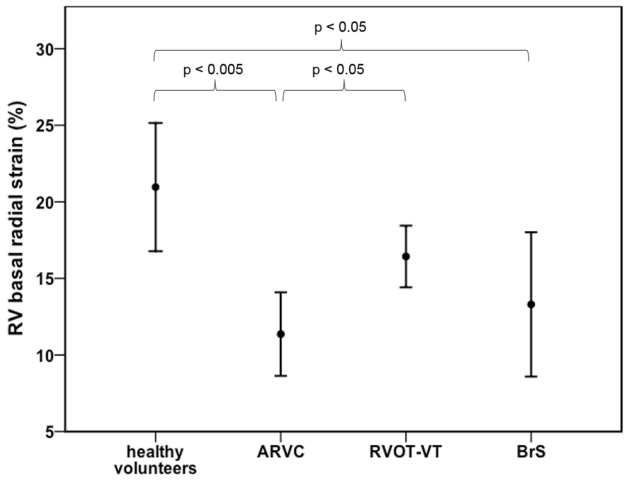

Fig. 3 Comparison of RV basal radial strain between HV and patient groups

reduced ($p \leq 0.05$) in comparison to HV (20.1 ± 6.6), supplementary (Fig. 6; Table 4).

ROC analysis

On RV strain-based ROC analysis between ARVC and HV (Table 5) as well as between ARVC and RVOT-VT (Table 5; Fig. 7a) RV longitudinal strain, on corresponding ROC analysis between BrS and HV (Table 6; Fig. 7b) RV medial radial strain proved to be the best discriminators (AUC 0.94, 0.88, 0.86).

On LV strain-based ROC analysis between ARVC and HV (Table 5; Fig. 7c) LV longitudinal strain, on corresponding ROC analysis between BrS and HV (Table 6; Fig. 7d) LV

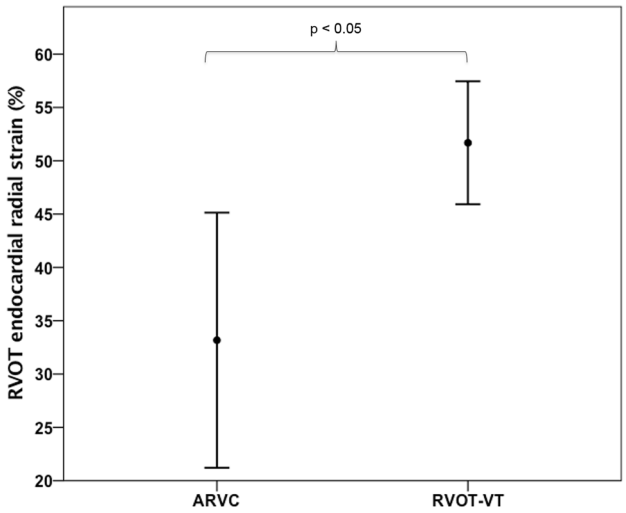

Fig. 4 Comparison of RVOT endocardial radial strain between HV and patient groups

Interobserver analysis

According to compared CMR-based strain parameters (Table 7), we did not find significant differences between the values of the experienced and the unexperienced reader. Correlation values of our study can be classified as proving a strong positive agreement between the readers' results, as exemplarily implemented correlation for RV longitudinal strain was 0.7 (based on Pearson's *r* correlation) (Table 7; Fig. 8).

Discussion

Prior echocardiographic studies by Teske et al. and Aneq et al. have demonstrated the feasibility of application of RV strain imaging regarding the diagnostic workup of suspected ARVC [42–44].

Due to the predominant use of CMR nowadays in clinical routine for cardiomyopathies, its determinative role in diagnostic workup of ARVC [1, 9–11] and due to the prior implementation of a FT algorithm retrospectively deriving strain parameters from conventional cine CMR images in basal radial strain was ascertained as the best discriminators (AUC: 0.93; 0.94), whereas corresponding values of LVEF were markedly lower, respectively (AUC: 0.53; 0.61).

Table 3 Comparison of right ventricular outflow tract strain and strainrate parameters between healthy volunteers, ARVC, RVOT-VT, and BrS

	Healthy volunteers	ARVC	RVOT-VT	BrS
RVOT endocardial strain (%)				
Longitudinal	−21.6 ± 5.2	−17.3 ± 8.3	−22.6 ± 4.9	−21.7 ± 3.6
Radial	46.6 ± 15.0	33.8 ± 22.7#	54.3 ± 14.5	44.8 ± 13.5
RVOT endocardial strainrate (1/s)				
Longitudinal	−1.55 ± 0.48	−1.22 ± 0.64	−1.60 ± 0.50	−1.51 ± 0.45
Radial	4.61 ± 4.10	1.86 ± 1.18#	2.99 ± 0.94	2.31 ± 0.49

ARVC arrhythmogenic right ventricular cardiomyopathy, *RVOT-VT* right ventricular outflow tract tachycardia, *BrS* Brugada syndrome; *RVOT* right ventricular outflow tract

Level of significance #$p < 0.05$

#Significant difference compared to patients with RVOT-VT

Table 4 Comparison of right ventricular strain parameters between subgroups: healthy volunteers, ARVC EF > 40%, RVOT-VT, and BrS EF > 45%

	Healthy volunteers	ARVC EF > 40% ($n = 9$)	RVOT-VT	BrS EF > 45% ($n = 6$)
RV strain (%)				
Longitudinal	−20.1 ± 3.7	−14.6 ± 3.1**#	−17.9 ± 2.5	−17.8 ± 2.2
Radial				
Basal	21.0 ± 6.9	13.8 ± 3.5*	16.8 ± 4.9	14.7 ± 6.6
Medial	20.1 ± 6.6	15.5 ± 7.4	13.3 ± 5.4	12.0 ± 2.7*

ARVC EF > 40% arrhythmogenic right ventricular cardiomyopathy with ejection fraction > 40%, *RVOT-VT* right ventricular outflow tract tachycardia, *BrS EF* > 45% Brugada syndrome with ejection fraction > 45%

Level of significance *,#$p < 0.05$,**$p < 0.01$

*Significant difference compared to healthy volunteers

#Significant difference compared to patients with RVOT-VT

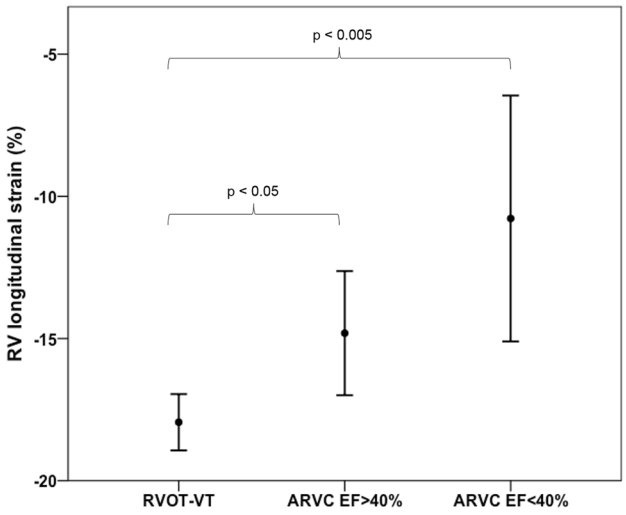

Fig. 5 Comparison of RV longitudinal strain between RVOT-VT and ARVC patient subgroups divided based on RVEF > or < 40%

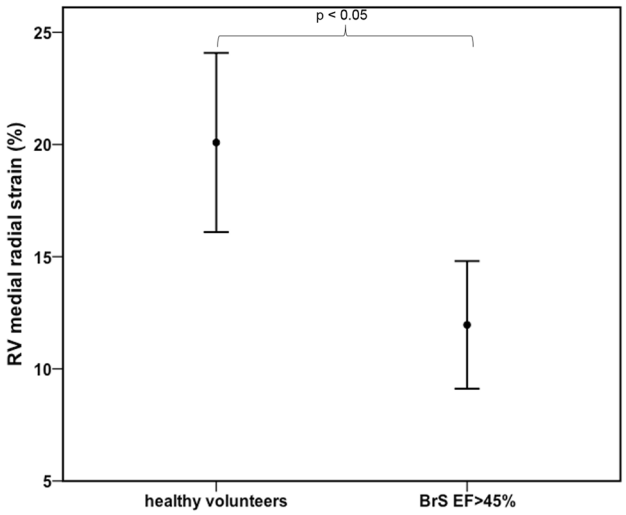

Fig. 6 Comparison of RV medial radial strain between HV and BrS patient subgroup with a RVEF > 45%

accordance with Hor et al. [30, 31], we recently assessed the reliability of CMR-FT for differentiation of ARVC from HV [12]. As sequel to these results, we currently examined the diagnostic performance of CMR-FT in the domain of leading differential diagnoses of ARVC.

Regarding BrS so far, in accordance with Antzelevitch et al., Wilde et al. and Brugada et al. ventricular tachyarrhythmias of right bundle branch block (RBBB) morphology and its characteristic Type-1-ECG are supposed to be unrelated to identifiable phenotypic myocardial changes in CMR [4, 5, 23, 24]. The absence of pathomorphological tissue characteristics in BrS further was affirmed by a study based on conventional quantitative functional as well as qualitative CMR parameters by Tessa et al. [45]. Despite these conventional quantitative findings being additionally appropriate to conventional functional results of our current study except for RVEF (Table 1), we found both RV basal circumferential, RV basal and medial radial strain as well as LV basal radial strain in BrS to be significantly reduced compared to HV. These results emphasize a high sensitivity of CMR strain for subtle deteriorations of myocardial function in diagnostic workup of BrS (Table 2; Fig. 3). Despite feasibility and performance of echocardiographic-based strain imaging using 2D speckle tracking in BrS has been examined by Iacoviello et al. and Murata et al. previously [29, 46], performance of CMR-based strain using FT in BrS has not been examined yet. In this context we further found RV medial radial strain within a subgroup analysis of BrS with a preserved RVEF (> 45%) to be significantly reduced in comparison to HV (Table 4; Fig. 6) implicating a superior sensitivity of CMR strain parameters compared to conventional functional measures. In this context also LV basal radial strain proved to significantly differentiate BrS from HV (Table 2).

Feasibility of strain measurements of the left ventricle by CMR FT in context with several cardiac diseases has been proven by numerous studies, as for instance by Buckert et al. [47].

Findings for LV strain parameters in BrS proved to be largely parallel to our current findings for CMR-FT in ARVC, as LV longitudinal strain and strainrate as well as LV basal radial strainrate in ARVC proved to be significantly reduced when compared to healthy volunteers (Table 2). Our findings are in line with results regarding LV involvement in patients with ARVC by teRiele et al., SenChowdhry et al. and Jain et al. [1, 48, 49].

Our findings further emphasize a superior accuracy of LV CMR-FT compared to conventional LV functional measures in BrS and ARVC, as LV volumetry did not differ between the four study groups resulting in AUC of only 0.61 (LVEF) versus 0.94 for LV basal radial strain in comparison on HV and BrS and resulting in AUC of only 0.53 (LVEF) versus 0.93 for LV longitudinal strain in comparison of HV and ARVC.

In accordance with Prati et al. [40], RV longitudinal and RV radial strain at the basal level in ARVC proved to be significantly decreased compared with corresponding values of RVOT-VT (Table 2; Figs. 2, 3).

We further performed a subgroup analysis based on EF cutoff values for ARVC and found that RV longitudinal strain even was significantly reduced in ARVC cases with a solely slightly reduced or even preserved EF > 40% compared to RVOT-VT (Table 4; Fig. 5). This fact further emphasizes high sensitivity of CMR-FT for detection of early disease stages of ARVC in direct comparison to RVOT-VT.

Concerning developing changes in the paradigm of the ARVC-related triangle of dysplasia with predominant focus

Table 5 Receiver operating curve characteristics: comparison of HV and ARVC as well as of RVOT-VT and ARVC

	AUC	Significance	Lower 95% CL	Upper 95% CL	Cut-off	Sensitivity (%)	Specificity (%)
HV vs. ARVC							
RV EF (%)	0.94	0.0003	0.84	1.0	51.4	94	100
RV strain (%)							
Longitudinal	0.94	0.0004	0.83	1.0	− 17.1	94	89
Circumferential							
Basal	0.87	0.003	0.68	1.0	− 12.4	94	78
Medial	0.83	0.007	0.67	0.99	− 13.3	88	67
Radial							
Basal	0.90	0.001	0.77	1.0	16.7	81	78
RV strainrate (1/s)							
Circumferential							
Basal	0.80	0.025	0.55	1.0	− 0.69	92	75
Radial							
Basal	0.82	0.017	0.62	1.0	1.03	83	75
Medial	0.80	0.025	0.60	1.0	1.15	83	62
LV EF (%)	0.53	0.79	0.30	0.77	64.8	73	33
LV strain (%)							
Longitudinal	0.93	0.001	0.81	1.0	− 18.3	93	89
RVOT-VT vs. ARVC							
RV EF (%)	0.88	0.000032	0.76	1.0	46.7	88	85
RV strain (%)							
Longitudinal	0.88	0.000047	0.77	0.98	− 16.5	88	70
Radial							
Basal	0.78	0.003	0.63	0.92	15.1	75	70
RVOT endocardial strain (%)							
Radial	0.76	0.008	0.59	0.93	55.4	79	58
RVOT endocardial strainrate (1/s)							
Radial	0.79	0.004	0.62	0.97	2.21	77	80

AUC area under the curve (95% CL—confidence levels) for conventional right and left ventricular ejection fraction (RVEF, LVEF), right (RV) and left ventricular (LV) as well as right ventricular outflow tract (RVOT) strain and strainrate parameters in comparison of HV and ARVC as well as of RVOT-VT and ARVC

HV healthy volunteers, *ARVC* arrhythmogenic right ventricular cardiomyopathy, *RVOT-VT* right ventricular outflow tract tachycardia

$p < 0.05$.optimal cutoff values of conventional RV and LV EF and of RV, LV and RVOT strain and strainrate parameters and corresponding levels of sensitivity and specificity, respectively

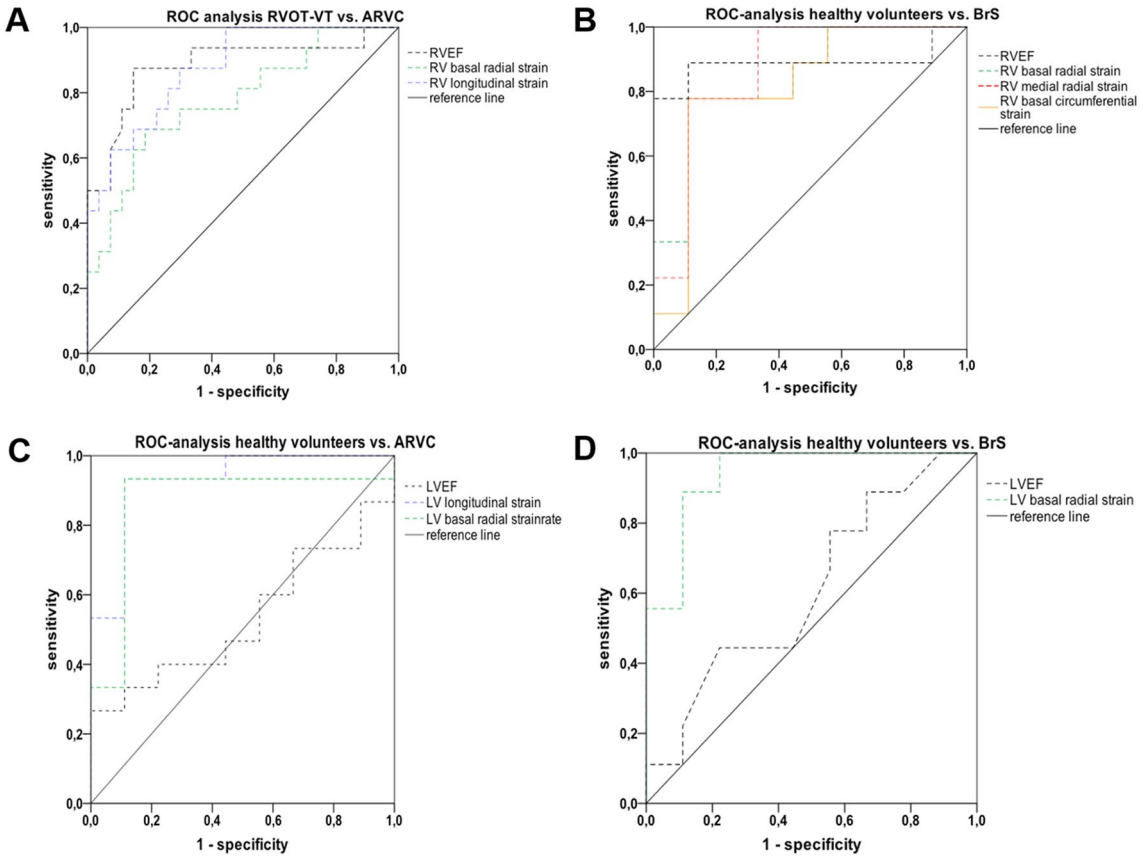

Fig. 7 Receiver operating curves (ROC) of selected RV (**a, b**) and LV (**c, d**) conventional functional and strain parameters for differentiating RVOT-VT from ARVC (**a**), HV from BrS (**b, d**) and HV from ARVC (**c**)

on the subtricuspid region and the RVOT but simultaneously ruled out apical region [1], so far, CMR-FT at the RVOT level has not been examined yet.

In addition to Prati et al. [40], we therefore investigated the performance of RV strain analysis at RVOT level in patients with RV tachyarrhythmias. Corresponding RVOT endocardial radial strain and strainrate in ARVC were found to be significantly reduced compared to RVOT-VT underlining RVOT strain values as further promising parameters for differentiation of RV tachyarrhythmias (Table 3; Fig. 4).

In addition to Heermann et al. [12], we currently included age-matched study groups and ascertained longitudinal strain parameters based on a 4-CH view adjusted to the cardiac axis for standardized acquisition [12].

A marked improvement of the accuracy of RV longitudinal strain and its ascendency in direct comparison with RV circumferential or radial strains at the basal section in our actual study (AUC: 0.94 vs. 0.87 or 0.90; Table 5) can be interpreted by the changed 4-CH orientation.

Furthermore, on ROC analysis in comparison of both HV against ARVC and RVOT-VT against ARVC we found current strain parameters to be of superior accuracy in comparison to corresponding strainrate parameters [12].

Strainrate is defined as myocardial deformation with respect to time and therefore might be influenceable by relatively limited temporal resolution of CMR cine data resulting in decreased reproducibility [32].

In addition to Heermann et al. [12], we found that medial RV circumferential strain and medial RV radial strainrate in ARVC were significantly decreased compared to HV, whereas RV strain parameters at the apical level still did not significantly differ in our studies.

These results can be interpreted as synergistic to developing changes in the paradigm of the ARVC-related triangle of dysplasia, as structural changes in ARVC are found to be predominantly located in the subtricuspid region and the RV free wall regionally represented by RV basal strains. The apex by contrast proved to be spared from structural alterations compliant with teRiele et al. [1, 50].

Our current results for subgroup analysis are in line with a number of echocardiographic studies of subclinical myocardial diseases by Kang et al., Hilde et al., Tadic et al., Zoroufian et al. and Saccheri et al. [15–19], as RV longitudinal and RV basal radial strain even proved to be significantly reduced in ARVC with simultaneously solely slightly decreased or preserved EF (> 40%) (Table 4).

Table 6 Receiver operating curve characteristics: comparison of HV and BrS as well as of ARVC and BrS

	AUC	Significance	Lower 95% CL	Upper 95% CL	Cut-off	Sensitivity (%)	Specificity (%)
HV vs. BrS							
RV EF (%)	0.89	0.005	0.70	1.0	55.0	89	89
RV strain (%)							
Circumferential							
Basal	0.82	0.024	0.60	1.0	− 11.1	78	89
Radial							
Basal	0.84	0.015	0.65	1.0	14.9	78	89
Medial	0.86	0.009	0.68	1.0	13.4	78	89
LV EF (%)	0.61	0.43	0.34	0.88	61.5	67	44
LV strain (%)							
Radial							
Basal	0.94	0.002	0.83	1.0	29.3	89	89
ARVC vs. BrS							
RV EF (%)	0.77	0.027	0.59	0.95	44.0	69	67
RV strain (%)							
Longitudinal	0.79	0.017	0.61	0.98	− 16.0	75	67

AUC area under the curve (95% CL—confidence levels) for conventional right and left ventricular ejection fraction (RVEF, LVEF), right (RV) and left ventricular (LV) strain parameters in comparison of HV and BrS as well as ARVC and BrS

HV healthy volunteers, *ARVC* arrhythmogenic right ventricular cardiomyopathy, *BrS* Brugada syndrome

$p < 0.05$ optimal cut off values of conventional RV and LV EF and of RV and LV strain parameters and corresponding levels of sensitivity and specificity, respectively

Table 7 Interobserver analysis of CMR-FT-derived strain values

	n	Observer 1	Observer 2	Pearson's *r* correlation	Significance
RV strain (%)					
Longitudinal	57	− 16.4 ± 3.7	− 18.6 ± 4.6	0.70	$p < 0.005$
Radial					
Basal	57	14.6 ± 5.6	16.3 ± 8.1	0.64	$p < 0.005$
Medial	57	13.6 ± 6.7	15.3 ± 6.3	0.45	$p < 0.005$
Apical	57	24.1 ± 12.5	24.8 ± 11.5	0.59	$p < 0.005$
RVOT endocardial strain (%)					
Radial	54	46.2 ± 18.8	40.3 ± 17.0	0.55	$p < 0.005$

Interobserver analysis of CMR-FT-derived strain values for right ventricular (RV) longitudinal and radial strains as well as for right ventricular outflow tract (RVOT) endocardial radial strain based on Pearson's *r* correlation

$p < 0.05$; observer 1 experienced; observer 2 unexperienced

Limitations

The results of the current study can only be interpreted for current usage of a special CMR deformation software (Circle Cardiovascular Imaging cvi[42], Canada and the Netherlands). Thus, conclusions regarding comparable or different results for CMR-FT of corresponding study groups with tachyarrhythmias of the RV using different deformation software tools, e.g., Diogenes MRI, Tomtec, Germany [12] cannot be drawn yet.

Furthermore, our current results are still based on a relatively small number of ARVC, RVOT-VT, and BrS patients due to the epidemiologic low prevalences of these rare cardiac diseases. Among the four patient groups, we did not control for the time of disease onset or definite diagnosis in relation to the timing of the CMR exam possibly resulting in a variation of disease durations both between patients of each study group and between groups.

Due to the fact that no echocardiographic strain analyses have been performed, a direct comparison of both methods with respect to their diagnostic value is still missing. Thus, no conclusive statement can be made regarding superiority of the diagnostic accuracy of either imaging modality. While Teske et al. [43] reported slightly higher values of AUC for global and segmental RV strain values, Aneq et al. [44] reported that longitudinal strain measurements using speckle tracking may be less reliable in more advanced disease stages of ARVC.

Our results were not controlled for the treatment with antiarrhythmic drugs. In this context Murata et al. found that echocardiographic strain measures in BrS were significantly reduced under the application of a sodium channel blocker [46].

Conclusion

We were able to demonstrate that CMR-FT may serve as a valuable tool to detect and quantify impaired myocardial function in BrS in addition to ARVC beyond conventional functional parameters, respectively.

CMR-FT-derived strain measures allowed for the differentiation between ARVC and HV or RVOT-VT as well as between HV and BrS. In this context even in patients with a solely slightly decreased (ARVC) or preserved EF (BrS) strain measures were found to be significantly impaired resulting in a superior accuracy of CMR-FT in comparison to conventional functional measures.

In view of these findings CMR-FT analysis constitutes a powerful measure to further objectify diagnosis of ARVC and BrS resulting in reliable detection of suspected cases of

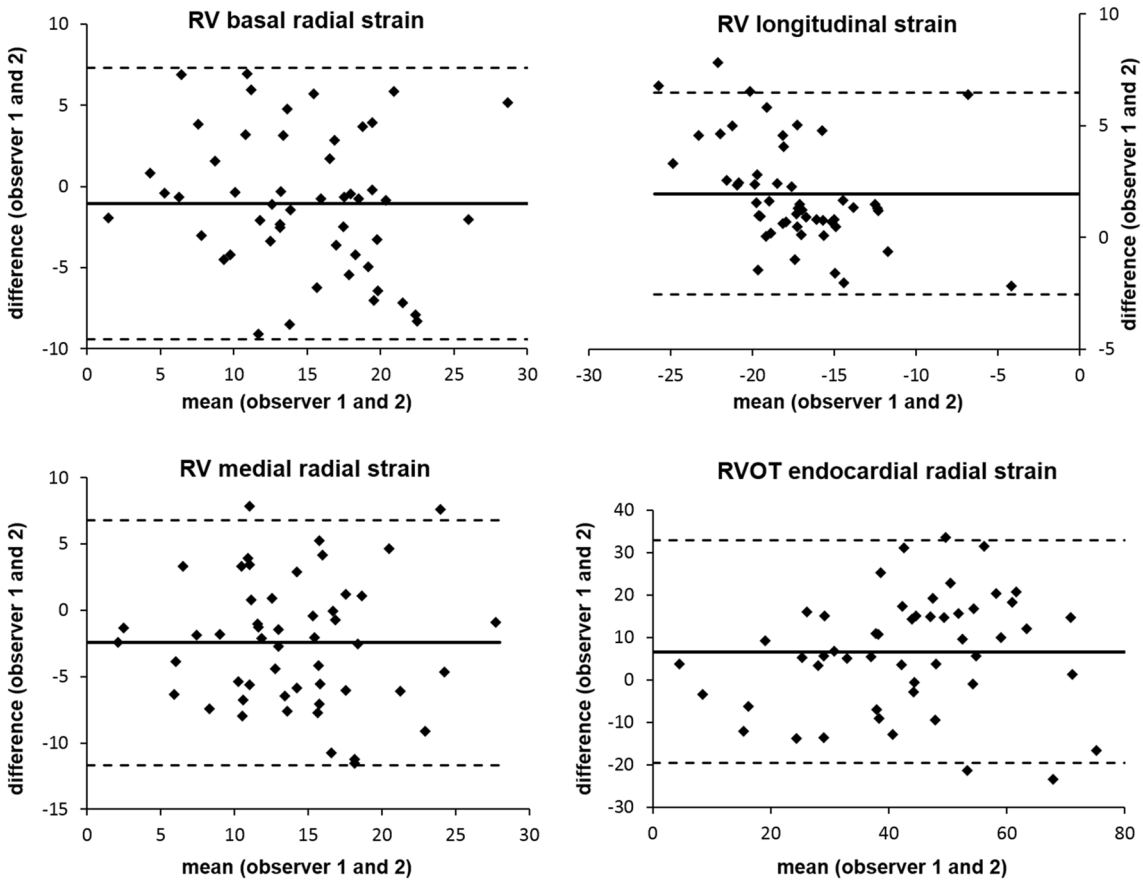

Fig. 8 Bland–Altman-plots of selected RV and RVOT strain parameters for interobserver analysis; black line: mean of differences; black dashed lines: mean of differences ± 1.96 multiplied by standard deviation (SD)

heart diseases of RV tachyarrhythmias that are in need for further specific therapy and careful follow-up.

Author contributions WH, ESB and PH initiated the study concept. PH is the corresponding author of the manuscript. PH and HF participated in the myocardial strain analysis. PH and CS participated in the statistical analysis and PH and CS drafted the manuscript. WH, ESB, MP, HF, MK and PS contributed valuable comments and formulations. All authors read and approved the final manuscript.

Compliance with ethical standards

Conflict of interest The authors declare that they have no conflict of interest.

Ethical approval Institutional Review Board approval was obtained. The current study obtained approval and consent from the local ethics committee (ethics commission of the medical association Westfalen-Lippe and the medical faculty of the Westfälische-Wilhelms-University (WWU) Muenster; reference number: 2013-632-f-N).

Informed consent Written informed consent was obtained from all subjects (patients) prior to their inclusion in the study.

References

1. Riele te ASJM, Tandri H, Bluemke DA (2014) Arrhythmogenic right ventricular cardiomyopathy (ARVC): cardiovascular magnetic resonance update. J Cardiovasc Magn Reson 16:50. https://doi.org/10.1186/s12968-014-0050-8
2. Azaouagh A, Churzidse S, Konorza T, Erbel R (2011) Arrhythmogenic right ventricular cardiomyopathy/dysplasia: a review and update. Clin Res Cardiol 100:383–394. https://doi.org/10.1007/s00392-011-0295-2
3. Marcus FI, McKenna WJ, Sherrill D et al (2010) Diagnosis of arrhythmogenic right ventricular cardiomyopathy/dysplasia: proposed modification of the task force criteria. Circulation 121:1533–1541. https://doi.org/10.1161/CIRCULATIONAHA.108.840827
4. Antzelevitch C, Brugada P, Borggrefe M et al (2005) Brugada syndrome: report of the second consensus conference: endorsed by the heart rhythm society and the european heart rhythm association. Circulation 111:659–670
5. Wilde AAM, Antzelevitch C, Borggrefe M et al (2002) Proposed diagnostic criteria for the Brugada syndrome: consensus report. Circulation 106:2514–2519
6. Paul M, Schulze-Bahr E, Eckardt L et al (2005) Right ventricular tachyarrhythmias–diagnostics and therapy. Herzschrittmachertherther Elektrophysiol 16:260–269. https://doi.org/10.1007/s00399-005-0493-6

7. Basso C, Corrado D, Marcus FI et al (2009) Arrhythmogenic right ventricular cardiomyopathy. Lancet 373:1289–1300. https://doi.org/10.1016/S0140-6736(09)60256-7
8. McKenna WJ, Thiene G, Nava A et al (1994) Diagnosis of arrhythmogenic right ventricular dysplasia/cardiomyopathy. task force of the working group myocardial and pericardial disease of the european society of cardiology and of the scientific council on cardiomyopathies of the international society and federation of cardiology. Br Heart J 71:215–218
9. Fairbairn TA, Motwani M, Greenwood JP, Plein S (2012) CMR for the diagnosis of right heart disease. JACC Cardiovasc Imaging 5:227–229. https://doi.org/10.1016/j.jcmg.2011.09.023
10. Riele te ASJM, Tandri H, Sanborn DM, Bluemke DA (2015) Non-invasive multimodality imaging in ARVD/C. JACC Cardiovasc Imaging 8:597–611. https://doi.org/10.1016/j.jcmg.2015.02.007
11. Quarta G, Husain SI, Flett AS et al (2013) Arrhythmogenic right ventricular cardiomyopathy mimics: role of cardiovascular magnetic resonance. J Cardiovasc Magn Reson 15:16. https://doi.org/10.1186/1532-429X-15-16
12. Heermann P, Hedderich DM, Paul M et al (2014) Biventricular myocardial strain analysis in patients with arrhythmogenic right ventricular cardiomyopathy (ARVC) using cardiovascular magnetic resonance feature tracking. J Cardiovasc Magn Reson 16:75. https://doi.org/10.1186/s12968-014-0075-z
13. Marwick TH (2006) Measurement of strain and strain rate by echocardiography: ready for prime time? J Am Coll Cardiol 47:1313–1327. https://doi.org/10.1016/j.jacc.2005.11.063
14. Sutherland GR, Di Salvo G, Claus P et al (2004) Strain and strain rate imaging: a new clinical approach to quantifying regional myocardial function. J Am Soc Echocardiogr 17:788–802. https://doi.org/10.1016/j.echo.2004.03.027
15. Kang Y, Cheng L, Li L et al (2013) Early detection of anthracycline-induced cardiotoxicity using two-dimensional speckle tracking echocardiography. Cardiol J 20:592–599. https://doi.org/10.5603/CJ.2013.0158
16. Hilde JM, Skjørten I, Grøtta OJ et al (2013) Right ventricular dysfunction and remodeling in chronic obstructive pulmonary disease without pulmonary hypertension. J Am Coll Cardiol 62:1103–1111. https://doi.org/10.1016/j.jacc.2013.04.091
17. Tadic M, Majstorovic A, Pencic B et al (2014) The impact of high-normal blood pressure on left ventricular mechanics: a three-dimensional and speckle tracking echocardiography study. Int J Cardiovasc Imaging 30:699–711. https://doi.org/10.1007/s10554-014-0382-3
18. Zoroufian A, Razmi T, Taghavi-Shavazi M et al (2014) Evaluation of subclinical left ventricular dysfunction in diabetic patients: longitudinal strain velocities and left ventricular dyssynchrony by two-dimensional speckle tracking echocardiography study. Echocardiography 31:456–463. https://doi.org/10.1111/echo.12389
19. Saccheri MC, Cianciulli TF, Lax JA et al (2013) Two-dimensional speckle tracking echocardiography for early detection of myocardial damage in young patients with fabry disease. Echocardiography 30:1069–1077. https://doi.org/10.1111/echo.12216
20. Cusmà Piccione M, Zito C, Bagnato G et al (2013) Role of 2D strain in the early identification of left ventricular dysfunction and in the risk stratification of systemic sclerosis patients. Cardiovasc Ultrasound 11:6. https://doi.org/10.1186/1476-7120-11-6
21. Markowitz SM, Weinsaft JW, Waldman L et al (2014) Reappraisal of cardiac magnetic resonance imaging in idiopathic outflow tract arrhythmias. J Cardiovasc Electrophysiol 25:1328–1335. https://doi.org/10.1111/jce.12503
22. Decher N, Ortiz-Bonnin B, Friedrich C et al (2017) Sodium permeable and "hypersensitive" TREK-1 channels cause ventricular tachycardia. EMBO Mol Med 9:403–414. https://doi.org/10.15252/emmm.201606690
23. Brugada P, Brugada J (1992) Right bundle branch block, persistent ST segment elevation and sudden cardiac death: a distinct clinical and electrocardiographic syndrome: a multicenter report. J Am Coll Cardiol 20:1391–1396
24. Antzelevitch C, Nof E (2008) Brugada syndrome: recent advances and controversies. Curr Cardiol Rep 10:376–383
25. Brugada R, Brugada J, Antzelevitch C et al (2000) Sodium channel blockers identify risk for sudden death in patients with ST-segment elevation and right bundle branch block but structurally normal hearts. Circulation 101:510–515
26. Priori SG, Wilde AA, Horie M et al (2013) HRS/EHRA/APHRS expert consensus statement on the diagnosis and management of patients with inherited primary arrhythmia syndromes: document endorsed by HRS, EHRA, and APHRS in May 2013 and by ACCF, AHA, PACES, and AEPC in June 2013. Heart Rhythm 10:1932–1963. https://doi.org/10.1016/j.hrthm.2013.05.014
27. Catalano O, Antonaci S, Moro G et al (2009) Magnetic resonance investigations in Brugada syndrome reveal unexpectedly high rate of structural abnormalities. Eur Heart J 30:2241–2248. https://doi.org/10.1093/eurheartj/ehp252
28. Rudic B, Schimpf R, Veltmann C et al (2016) Brugada syndrome: clinical presentation and genotype-correlation with magnetic resonance imaging parameters. Europace 18:1411–1419. https://doi.org/10.1093/europace/euv300
29. Iacoviello M, Forleo C, Puzzovivo A et al (2011) Altered two-dimensional strain measures of the right ventricle in patients with Brugada syndrome and arrhythmogenic right ventricular dysplasia/cardiomyopathy. Eur J Echocardiogr 12:773–781. https://doi.org/10.1093/ejechocard/jer139
30. Hor KN, Gottliebson WM, Carson C et al (2010) Comparison of magnetic resonance feature tracking for strain calculation with harmonic phase imaging analysis. JACC Cardiovasc Imaging 3:144–151. https://doi.org/10.1016/j.jcmg.2009.11.006
31. Hor KN, Baumann R, Pedrizzetti G et al (2011) Magnetic resonance derived myocardial strain assessment using feature tracking. J Vis Exp. https://doi.org/10.3791/2356
32. Orwat S, Kempny A, Diller G-P et al (2014) Cardiac magnetic resonance feature tracking: a novel method to assess myocardial strain. Comparison with echocardiographic speckle tracking in healthy volunteers and in patients with left ventricular hypertrophy. Kardiol Pol 72:363–371. https://doi.org/10.5603/KP.a2013.0319
33. Kempny A, Fernández-Jiménez R, Orwat S et al (2012) Quantification of biventricular myocardial function using cardiac magnetic resonance feature tracking, endocardial border delineation and echocardiographic speckle tracking in patients with repaired tetralogy of fallot and healthy controls. J Cardiovasc Magn Reson 14:32. https://doi.org/10.1186/1532-429X-14-32
34. Kempny A, Diller G-P, Orwat S et al (2012) Right ventricular-left ventricular interaction in adults with tetralogy of fallot: a combined cardiac magnetic resonance and echocardiographic speckle tracking study. Int J Cardiol 154:259–264. https://doi.org/10.1016/j.ijcard.2010.09.031
35. Schuster A, Kutty S, Padiyath A et al (2011) Cardiovascular magnetic resonance myocardial feature tracking detects quantitative wall motion during dobutamine stress. J Cardiovasc Magn Reson 13:58. https://doi.org/10.1186/1532-429X-13-58
36. Schuster A, Paul M, Bettencourt N et al (2013) Cardiovascular magnetic resonance myocardial feature tracking for quantitative viability assessment in ischemic cardiomyopathy. Int J Cardiol 166:413–420. https://doi.org/10.1016/j.ijcard.2011.10.137
37. Maret E, Todt T, Brudin L et al (2009) Functional measurements based on feature tracking of cine magnetic resonance images identify left ventricular segments with myocardial scar. Cardiovasc Ultrasound 7:53. https://doi.org/10.1186/1476-7120-7-53

38. Kutty S, Rangamani S, Venkataraman J et al (2013) Reduced global longitudinal and radial strain with normal left ventricular ejection fraction late after effective repair of aortic coarctation: a CMR feature tracking study. Int J Cardiovasc Imaging 29:141–150. https://doi.org/10.1007/s10554-012-0061-1
39. Vigneault DM, Riele te ASJM, James CA et al (2015) Right ventricular strain by MR quantitatively identifies regional dysfunction in patients with arrhythmogenic right ventricular cardiomyopathy. J Magn Reson Imaging 43:1132–1139. https://doi.org/10.1002/jmri.25068
40. Prati G, Vitrella G, Allocca G et al (2015) Right ventricular strain and dyssynchrony assessment in arrhythmogenic right ventricular cardiomyopathy: cardiac magnetic resonance feature-tracking study. Circ Cardiovasc Imaging. https://doi.org/10.1161/CIRCIMAGING.115.003647
41. Marcus FI, McKenna WJ, Sherrill D et al (2010) Diagnosis of arrhythmogenic right ventricular cardiomyopathy/dysplasia: proposed modification of the Task Force Criteria. Eur Heart J 31(7):806–814
42. Teske AJ, Cox MGPJ, Riele te ASJM et al (2012) Early detection of regional functional abnormalities in asymptomatic ARVD/C gene carriers. J Am Soc Echocardiogr 25:997–1006. https://doi.org/10.1016/j.echo.2012.05.008
43. Teske AJ, Cox MG, De Boeck BW et al (2009) Echocardiographic tissue deformation imaging quantifies abnormal regional right ventricular function in arrhythmogenic right ventricular dysplasia/cardiomyopathy. J Am Soc Echocardiogr 22:920–927. https://doi.org/10.1016/j.echo.2009.05.014
44. Aneq M, Engvall J, Brudin L, Nylander E (2012) Evaluation of right and left ventricular function using speckle tracking echocardiography in patients with arrhythmogenic right ventricular cardiomyopathy and their first degree relatives. Cardiovasc Ultrasound 10:37. https://doi.org/10.1186/1476-7120-10-37
45. Tessa C, Del Meglio J, Ghidini Ottonelli A et al (2012) Evaluation of Brugada syndrome by cardiac magnetic resonance. Int J Cardiovasc Imaging 28:1961–1970. https://doi.org/10.1007/s10554-012-0009-5
46. Murata K, Ueyama T, Tanaka T et al (2011) Right ventricular dysfunction in patients with Brugada-like electrocardiography: a two dimensional strain imaging study. Cardiovasc Ultrasound 9:30. https://doi.org/10.1186/1476-7120-9-30
47. Buckert D, Cieslik M, Tibi R et al (2017) Longitudinal strain assessed by cardiac magnetic resonance correlates to hemodynamic findings in patients with severe aortic stenosis and predicts positive remodeling after transcatheter aortic valve replacement. Clin Res Cardiol 107:20–29. https://doi.org/10.1007/s00392-017-1153-7
48. Sen-Chowdhry S, Syrris P, Prasad SK et al (2008) Left-dominant arrhythmogenic cardiomyopathy: an under-recognized clinical entity. J Am Coll Cardiol 52:2175–2187. https://doi.org/10.1016/j.jacc.2008.09.019
49. Jain A, Shehata ML, Stuber M et al (2010) Prevalence of left ventricular regional dysfunction in arrhythmogenic right ventricular dysplasia: a tagged MRI study. Circ Cardiovasc Imaging 3:290–297. https://doi.org/10.1161/CIRCIMAGING.109.911313
50. Riele te ASJM, James CA, Philips B et al (2013) Mutation-positive arrhythmogenic right ventricular dysplasia/cardiomyopathy: the triangle of dysplasia displaced. J Cardiovasc Electrophysiol 24:1311–1320. https://doi.org/10.1111/jce.12222

Affiliations

Philipp Heermann[1] · H. Fritsch[5] · M. Koopmann[3] · P. Sporns[2] · M. Paul[4] · W. Heindel[2] · E. Schulze-Bahr[5] · C. Schülke[2]

H. Fritsch
hanna.fritsch@ukmuenster.de

M. Koopmann
matthias.koopmann@ukmuenster.de

P. Sporns
peter.sporns@ukmuenster.de

M. Paul
matthias.paul@ukmuenster.de

W. Heindel
heindel@uni-muenster.de

E. Schulze-Bahr
eric.schulze-bahr@ukmuenster.de

C. Schülke
christoph.schuelke@ukmuenster.de

[1] Center of Radiology, Neuroradiology and Nuclear Medicine, Clemens Hospital Muenster, Duesbergweg 124, 48153 Muenster, Germany

[2] Department of Clinical Radiology, University Hospital Muenster, Muenster, Germany

[3] Department of Cardiology and Angiology, University Hospital Muenster, Muenster, Germany

[4] Division of Cardiology, Department of Cardiovascular Medicine, University Hospital Muenster, Muenster, Germany

[5] Institute for Genetics of Heart Diseases, Department of Cardiovascular Medicine, University Hospital Muenster, Muenster, Germany